JACS
JOURNAL OF THE AMERICAN CHEMICAL SOCIETY
Article
pubs.acs.org/JACS

Identification of a Key Catalytic Intermediate Demonstrates That Nitrogenase Is Activated by the Reversible Exchange of N_2 for H_2

Dmitriy Lukoyanov,[‡,∥] Zhi-Yong Yang,[†,∥] Nimesh Khadka,[†] Dennis R. Dean,[*,§] Lance C. Seefeldt,[*,†] and Brian M. Hoffman[*,‡]

[‡]Departments of Chemistry and Molecular Biosciences, Northwestern University, Evanston, Illinois 60208, United States
[†]Department of Chemistry and Biochemistry, Utah State University, Logan, Utah 84322, United States
[§]Department of Biochemistry, Virginia Tech, Blacksburg, Virginia 24061, United States

Supporting Information

ABSTRACT: Freeze-quenching nitrogenase during turnover with N_2 traps an $S = {}^1/_2$ intermediate that was shown by ENDOR and EPR spectroscopy to contain N_2 or a reduction product bound to the active-site molybdenum–iron cofactor (FeMo-co). To identify this intermediate (termed here ***EG***), we turned to a quench-cryoannealing relaxation protocol. The trapped state is allowed to relax to the resting E_0 state in frozen medium at a temperature below the melting temperature; relaxation is monitored by periodically cooling the sample to cryogenic temperature for EPR analysis. During −50 °C cryoannealing of ***EG*** prepared under turnover conditions in which the concentrations of N_2 and H_2 ($[H_2]$, $[N_2]$) are systematically and independently varied, the rate of decay of ***EG*** is accelerated by increasing $[H_2]$ and slowed by increasing $[N_2]$ in the frozen reaction mixture; correspondingly, the accumulation of ***EG*** is greater with low $[H_2]$ and/or high $[N_2]$. The influence of these diatomics identifies ***EG*** as the key catalytic intermediate formed by reductive elimination of H_2 with concomitant N_2 binding, a state in which FeMo-co binds the components of diazene (an N–N moiety, perhaps N_2 and two $[e^-/H^+]$ or diazene itself). This identification combines with an earlier study to demonstrate that nitrogenase is activated for N_2 binding and reduction through the thermodynamically and kinetically reversible reductive-elimination/oxidative-addition exchange of N_2 and H_2, with an implied limiting stoichiometry of eight electrons/protons for the reduction of N_2 to two NH_3.

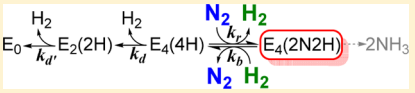

INTRODUCTION

Biological nitrogen fixation—the reduction of N_2 to two NH_3 molecules—is primarily catalyzed by the Mo-dependent nitrogenase. This enzyme comprises an electron-delivery Fe protein and MoFe protein, a dimer of dimers that contains two copies of the active-site FeMo-cofactor (FeMo-co).[1,2] A suggested limiting stoichiometry for nitrogen fixation,[3]

$$N_2 + 8e^- + 16ATP + 8H^+ \rightarrow 2NH_3 + H_2 + 16ADP + 16P_i \quad (1)$$

incorporates an obligatory formation of 1 mol of H_2 per mole of N_2 reduced, and thus a puzzling requirement for two reducing equivalents and four ATP beyond the chemical requirement for N_2 reduction.[1,2] This stoichiometry is embodied in a kinetic framework for nitrogenase function provided by the Lowe–Thorneley (LT) model,[1,2,4] which describes transformations among catalytic intermediates denoted E_n, where n is the number of electrons and protons (n = 0–8) delivered to one-half of the MoFe protein (Figure 1A). In this model, N_2 reduction requires activation of the MoFe protein to the pivotal $E_4(4H)$ state (see the kinetic scheme of Figure 1, where the legend explains notation), in which ENDOR has shown FeMo-co to have accumulated four reducing equivalents stored in the form of two [Fe–H–Fe] bridging hydrides,[5−7] presumably with two protons bound to sulfides of FeMo-co (Figure 1B, left).[5,7−9] We recently proposed[8,10] and subsequently provided experimental evidence[11] that nitrogenase is activated for N_2 binding and reduction through reductive elimination (*re*)[12−15] of the two bridging hydrides of $E_4(4H)$ to form H_2 (Figure 1B), thereby experimentally supporting the stoichiometry of eq 1.

As part of the development of the *re* mechanism we used advanced paramagnetic techniques to characterize two nitrogenous E_n intermediates that are associated with states in the LT scheme subsequent to N_2 binding, $n \geq 4$ (Figure 1), and that are common to turnover of remodeled nitrogenase with N_2H_2, Me-N_2H, N_2H_4, NO_2^-, and H_2NOH. One is a non-Kramers ($S \geq 2$) state, denoted ***H***, that is assigned as E_7, with bound [-NH_2]; the second is a Kramers ($S = {}^1/_2$) state, denoted ***I***, assigned as E_8, with bound NH_3.[8,10,16] During turnover of wild-type nitrogenase with N_2 an additional intermediate state with $S = {}^1/_2$ was trapped, but not identified.[17−19] With a half-integer spin, like the E_0 resting state, this state must differ from E_0 by the accumulation of an n = even number of $[e^-/H^+]$ to FeMo-co. This state, herein denoted as ***EG***, must further correspond to an E_n state formed subsequent to binding N_2, n = 4, 6, or 8, because it gives ^{15}N ENDOR signals when trapped using $^{15}N_2$ substrate. The previous assignment of ***I*** as E_8, a product (NH_3)-bound state,[8,10] implies an assignment of ***EG*** to E_4 or E_6. The notation,

Received: January 5, 2015
Published: March 5, 2015

DOI: 10.1021/jacs.5b00103
J. Am. Chem. Soc. 2015, 137, 3610–3615

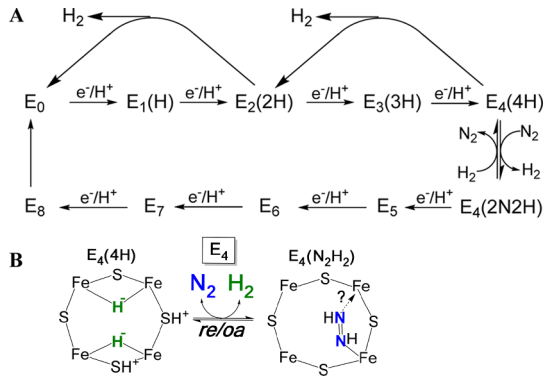

Figure 1. (A) Simplified LT kinetic scheme highlighting correlated electron/proton delivery in eight steps, with inclusion of some of the possible pathways for decay by H_2 release; although N_2 binds at either the E_3 or E_4 levels, only the E_4 state is reactive, so the pathway through the E_4 state is emphasized. For states under discussion in this report, parentheses added to the E_n notation to denote the stoichiometry of H/N bound to FeMo-co. When the molecular species corresponding to this stoichiometry is specified, it is noted; for example, $E_4(2N2H)$ might have N_2 or N_2H_2 bound, and would be notated as $E_4(N_2,2H)$ and $E_4(N_2H_2)$. (B) The reductive-elimination (*re*) mechanism for H_2 release upon N_2 (blue) binding to $E_4(4H)$ and its reverse, oxidative addition (*oa*) of H_2 with loss of N_2 (see eq 4) visualized as occurring on the Fe2,3,6,7 face of FeMo-co. The binding modes of the hydrides of $E_4(4H)$ and the components of diazene in $E_4(2N2H)$ are arbitrary.

EG, in fact was adopted because if the states of Figure 1A were to be labeled sequentially by letters beginning with E_0 = ***A***, then E_4 would be ***E*** and E_6 would be ***G***.

Because of the relatively low accumulation of ***EG*** in freeze-quenched samples, to date neither ENDOR measurements nor the use HYSCORE, as successfully applied to intermediate ***I***,[20] have yielded an assignment of ***EG***. To identify ***EG***, we therefore here turn to a quench-cryoannealing relaxation protocol developed to determine the reduction level, *n*, of an EPR-active freeze-trapped E_n intermediate state.[6] The trapped state is allowed to relax to the resting E_0 state in frozen medium, at temperatures $T \leq -20$ °C, well below the melting temperature of the buffered samples, $T \approx 0$ °C. Keeping the sample frozen prevents any additional accumulation of reducing equivalents, because binding of reduced Fe protein to and release of oxidized protein from the MoFe protein both are abolished in a frozen solid. As recently confirmed,[21] the frozen intermediate can relax toward the resting state only through steps that release a stable species from FeMo-co. The E_n states formed prior to N_2 binding lose 2 equiv per relaxation step by releasing H_2: $E_2(2H)$ relaxes to E_0 with loss of H_2; $E_3(3H)$ can relax to $E_1(1H)$ by loss of H_2, but as there is no center available to accept a single electron, $E_1(1H)$ cannot further relax to E_0;[21] E_4 is a special case with multiple substates (Figure 1B), which will be discussed. States formed subsequent to N_2 binding/reaction, $n > 4$, would relax through release of a stable form of reduced substrate. As the defining example of this approach, the freeze-trapped $S = {}^1/_2$ intermediate shown by ENDOR spectroscopy to exhibit two [Fe−H−Fe] bridging hydrides[5,7] was identified as $E_4(4H)$ by its relaxation to the resting state E_0 through the release of a total of four reducing equivalents in a two-step process, each step releasing H_2 (2 equiv), with formation of $E_2(2H)$ in the first step (Figure 1A).[6]

Application of this quench-cryoannealing relaxation protocol to ***EG*** identifies its E_n turnover state as one in which the N−N bond is intact. Most importantly, the results combine with our earlier study[11] to directly demonstrate that nitrogenase activation occurs as a thermodynamically *and* kinetically reductive-elimination/oxidative-addition (*re*/*oa*) exchange of N_2 and H_2 at the E_4 reduction level, as represented by Figure 1B.

MATERIALS AND METHODS

General Procedures. All chemicals were obtained from Sigma-Aldrich Chemicals, and were used without further purification. Hydrogen, argon, and dinitrogen gases were purchased from Air Liquide America Specialty Gases LLC (Plumsteadville, PA). The argon and dinitrogen gases were passed through an activated copper catalyst to get rid of contamination of oxygen before use. *Azotobacter vinelandii* strains DJ995 (wild-type MoFe protein) and DJ884 (wild-type Fe protein) were grown and nitrogenase proteins were expressed and purified as previously described.[22] Both proteins were greater than 95% pure as confirmed by SDS-PAGE analysis using Coomassie blue staining, and were fully active, as discussed in the Supporting Information (SI). Proteins and buffers were handled anaerobically in septum-sealed serum vials under an inert atmosphere (argon or dinitrogen) or on a Schlenk vacuum line. All transfers of gases and liquids were done with Hamilton gastight syringes.

Preparation of Cryoannealing Samples. Samples were prepared by adding Fe protein and MoFe protein to a solution containing a MgATP regeneration system, such that the final concentrations were 13 mM ATP, 15 mM $MgCl_2$, 20 mM phosphocreatine, 2.0 mg/mL bovine serum albumin, and 0.3 mg/mL phosphocreatine kinase (200 mM MOPS buffer at pH 7.3 with 50 mM dithionite). MoFe protein was added first to a final concentration of ∼50 μM; reaction was then initiated by the addition of Fe protein to a final concentration of ∼75 μM. After 20−25 s incubation at room temperature, ∼300 μL of the reaction mixture (total volume ∼400 μL) was transferred into 4 mm calibrated quartz EPR tubes and rapidly frozen in a hexane slurry before being stored in liquid nitrogen for EPR analysis. When effects of ammonium ion were studied, reaction mixtures contained a final ammonium chloride concentration of 0.2 mM.

To prepare unstirred samples with a selected N_2 partial pressure under normal conditions, N_2 (or Ar) gas was added to an argon (or N_2)-filled 9.4 mL assay vial with a 500 μL Eppendorf tube inside. The final pressure in all vials was 1 atm. When the stirring effect was studied, the assay vial contained a small magnetic stirring bar, the final volume of liquid phase was doubled to 0.8 mL, and the reaction mixture was stirred to equilibrate the gas and liquid phases. To study the effect of gas flushing in addition to stirring, the gas mixture with the chosen N_2 partial pressure in a 60 mL syringe was flushed through the headspace of the reaction vial from a syringe inserted through the water-sealed septum and ventilated through a second water-sealed small syringe attached through the septum; a total volume of 30 mL of gas mixture was flushed through the reaction vial prior to freezing. The NH_3, H_2 and N_2 concentrations in frozen samples prepared with the two protocols, unstirred and stirred, were estimated as described in SI (Figures S1−S3).

Cryoannealing EPR Methods. The cryoannealing protocol has been described.[6,21] It involves multiple steps in which a freeze-quenched sample at liquid nitrogen temperature is rapidly warmed to the annealing temperature by immersion in a methanol bath held at that temperature, annealed at that temperature for a fixed time, then quench-cooled back to 77 K by immersion into liquid nitrogen. CW X-band EPR is then collected on an ESP 300 Bruker spectrometer equipped with Oxford ESR 900 cryostat.

A freeze-trapped intermediate, E_n, typically decays with a distribution of rate constants, which can be described with a stretched exponential function, eq 2,[23]

$$E_n(t) \propto \exp(-(t/\tau)^m) \quad (2)$$

where τ is the average decay time and $0 \leq m \leq 1$ reflects the breadth of the distribution, with m decreasing as the breadth of the distribution increases.[24] In formulating the differential equations of a multistep

DOI: 10.1021/jacs.5b00103
J. Am. Chem. Soc. 2015, 137, 3610−3615

process, the distribution of rate constants that characterizes a stretched exponential decay is manifest as a time-dependent rate constant, $k(t)$.[6,24]

RESULTS AND DISCUSSION

Figure 2 (t = 0) presents the EPR spectrum of nitrogenase quench-frozen during steady-state turnover (ca. 25 s after

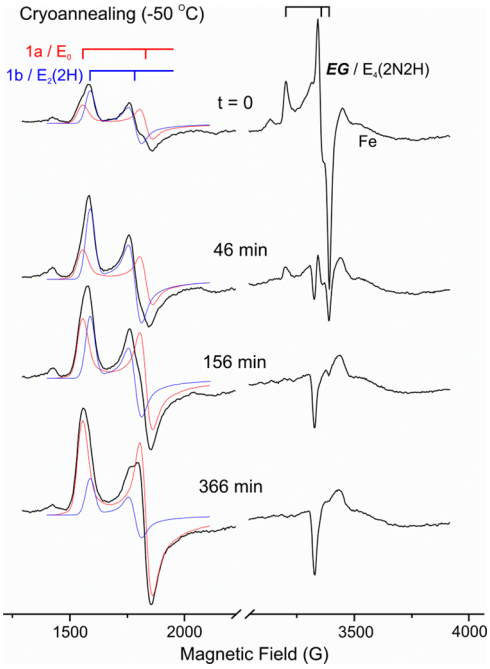

Figure 2. Selected EPR spectra collected during the time course for −50 °C cryoannealing of a sample freeze-trapped under $P(N_2)$ = 0.05 atm, and showing the decompositions of the $S = {}^3/_2$ spectra in the low-field g_1/g_2 region into contributions from 1a (**g** = [4.32, 3.66, 2.01], red) and 1b (**g** = [4.21, 3.76, ~1.97], blue). At early time the g_2 region is dominated by ***EG***, as indicated. The indicated signal from the reduced 4Fe/4S cluster of Fe protein is greatly distorted at this temperature, but it is clear that its intensity does not change with annealing. EPR conditions: temperature, 3.8 K; microwave frequency, 9.36 GHz; microwave power, 0.5 mW; modulation amplitude, 13 G; time constant, 160 ms; field sweep speed, 38 G/s.

mixing) under an N_2 partial pressure ($P(N_2)$) of 0.05 atm. At low fields it shows the g_1/g_2 features of $S = {}^3/_2$ signals, and is decomposed as previously described[21] (also see legend to Figure 3) into a contribution from the E_0 resting-state FeMo-co (signal denoted 1a), and a larger contribution from the E_2(2H) intermediate (denoted 1b).[6,21] The $g \sim 2$ region is dominated by the spectrum for the $S = {}^1/_2$ ***EG*** intermediate, **g** = [2.08, 1.99, 1.97].

Figure 2 further shows representative spectra collected during −50 °C cryoannealing of the freeze-trapped sample; the ***EG*** decay at higher annealing temperatures, (e.g., −20 °C) was too rapid to monitor conveniently. As shown, the annealing leads to progressive loss of the ***EG*** signal and increase in the E_0 signal, plus a rise then fall of the E_2 signal.

Figure 3A presents the progress curves for −50 °C cryoannealing of samples trapped during steady-state turnover both under $P(N_2)$ of 0.05 and 1 atm. As is commonly the case in cryoannealing,[6,23] the decay of ***EG*** formed under a partial pressure of $P(N_2)$ = 1 atm is best described with a stretched exponential,[24] eq 2, indicating that there is a distribution of rate

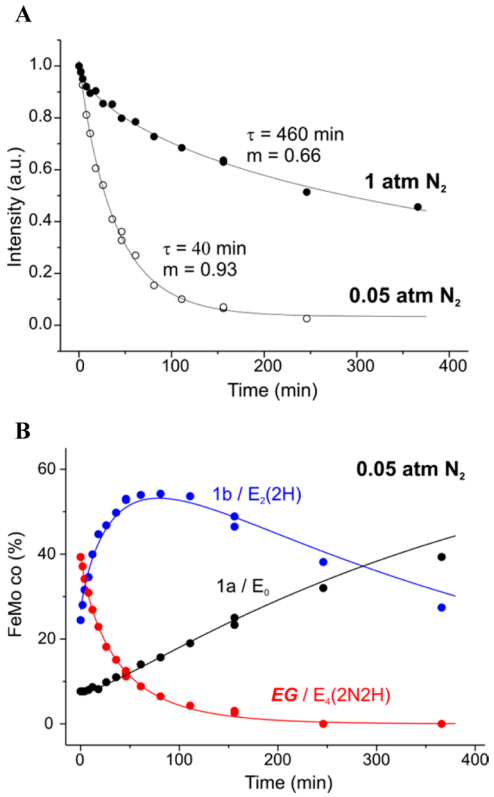

Figure 3. (A) Decay of intermediate ***EG*** freeze-trapped during turnover of nitrogenase under $P(N_2)$ = 0.05 (open circles; see Figure 2) and 1 atm (solid circles) observed during cryoannealing at −50 °C. Plotted are intensities of g_1 feature of the $S = {}^1/_2$ EPR signal, shown after normalization to the maximum (zero-time) signal and fitted with a stretched exponential decay function, eq 2. EPR conditions: as for Figure 2, except for field sweep speed of 20 G/s. (B) Progress curves for the three EPR-active species, ***EG***, 1a, and 1b, observed during cryoannealing of ***EG*** freeze-trapped under $P(N_2)$ = 0.05 atm. Fits to kinetic scheme (eq 3) as previously described; parameters of k_1 for ***EG*** stretched-exponential decay presented in panel A; rate of the second step of eq 3, k_2 = 0.0023 min^{-1}.[6,21] Intensities for the resting state (black) and E_2 state (blue) obtained with the previously described[21] procedure of deconvolution and quantitation of corresponding $S = {}^3/_2$ EPR signals 1a and 1b (see Figure 2). Intensities for the ***EG*** intermediate (red) taken from panel A and converted to concentration units by scaling to the two-step kinetic scheme for decay, eq 3. EPR conditions: as for panel A, except for field sweep speed of 38 G/s for 1a and 1b signals detection.

constants associated with an ensemble of slightly differing conformations of the intermediate trapped in the frozen solution. The decay at this temperature is slow, with an average decay time of τ = 460 min and a "stretch" constant, m = 0.66. Strikingly, when ***EG*** is trapped during turnover under an atmosphere of only $P(N_2)$ = 0.05 atm, the decay dramatically speeds up: the average decay time decreases more than 12-fold, to τ = 40 min; moreover, the decay becomes nearly exponential, m = 0.93.

As shown in Figure 2 and illustrated in 3B, decay of ***EG*** during cryoannealing leads to the appearance of the $S = {}^3/_2$ signal, denoted 1b, associated with the E_2(2H) intermediate.[6,21] This species in turn decays with the gradual recovery of resting state E_0. As ENDOR measurements show that ***EG*** is a state that has bound N_2,[8,10,16] and this state decays through E_2(2H) to E_0 during cryoannealing, then according to Figure 1A, ***EG*** can only be E_4(2N2H). According to this kinetic model, E_4(2N2H)

DOI: 10.1021/jacs.5b00103
J. Am. Chem. Soc. 2015, 137, 3610−3615

Scheme 1. Kinetic Scheme for the Decay of Freeze-Trapped $E_4(2N2H)$ Derived from Figure 1A[a]

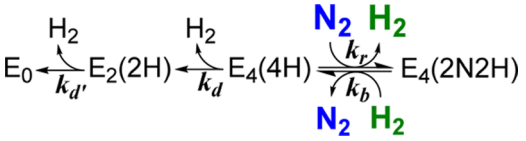

[a] k_r and k_b are the second-order rate constants for *re* and its reverse; k_d and k_d' are the rate constants for the irreversible[10] decay of $E_4(4H)$ and $E_2(2H)$, respectively.

relaxes via $E_4(4H)$ and $E_2(2H)$ to resting state E_0 with loss of N_2 and two H_2. This is described by Scheme 1, which extracts from Figure 1A those states associated with relaxation of $E_4(2N2H)$ to resting E_0. Multiple repetitions of the experiment, have shown that in general low amounts of an intermediate whose EPR signal can be assigned to $E_4(4H)$ are freeze-trapped, and that little to no additional $E_4(4H)$ accumulates during annealing. As a result of the latter in particular, the curves for all three observed species can be described jointly[6] by the phenomenological two-step sequential kinetic scheme derived from Scheme 1 under the condition of minimal accumulation of $E_4(4H)$, eq 3:

$$E_4(2N2H) \xrightarrow{k_1} E_2(2H) \xrightarrow{k_2} E_0 \qquad (3)$$

This implies a steady-state approximation for the concentration of $E_4(2N2H)$, presented below; the relationship between the observed ***EG***/$E_4(2N2H)$ decay constants, k_1, k_2, of eq 3, and the microscopic rate constants of Scheme 1 are derived there.

The progress curves for the three species, ***EG***/$E_4(2N2H)$, 1b/$E_2(2H)$, and 1a/E_0, are indeed well-fit by the kinetic relaxation scheme of eq 3, as illustrated for the sample trapped under $P(N_2)$ = 0.05 atm (Figure 3B). In agreement with this scheme, the appearance of 1b/$E_2(2H)$ follows the stretched-exponential (eq 2) associated with the decay of ***EG***, with changes in the partial pressure $P(N_2)$ causing the sharp changes in the average decay time and stretch factor that characterize k_1, as presented above. Correspondingly, 1a/E_0 appears with the rate constant associated with relaxation of 1b/$E_2(2H)$. In contrast, one expects the relaxation of $E_2(2H)$ to E_0 to be independent of turnover conditions,[6,21] and this is so. At both values of $P(N_2)$, the process can be described by an exponential with the same rate constant, implying that $k_2 = k_d'$ of Scheme 1.

The assignment of ***EG*** as $E_4(2N2H)$ has been tested, and confirmed, by experiments inspired by the question, why does *increasing* the concentration of the substrate $[N_2]$ in the frozen solution *slow* the decay of $E_4(2N2H)$ (Figure 3A), which led to the further questions, what are the possible influence(s) on ***EG*** decay of the turnover products, NH_3 and H_2? We first tested whether the NH_3 product (NH_4^+ at pH 7.3) is the causative agent, perhaps because it binds to MoFe in the vicinity of the FeMo-co of $E_4(2N2H)$ and stabilizes the intermediate, for example by H-bonding to a partially reduced N_2. As NH_3 production increases with increasing $P(N_2)$ (Figure S1), such an effect would be enhanced at high $P(N_2)$, thereby decreasing the rate of decay, as observed.

To test this hypothesis, we first quantified the ammonia concentration in the samples prepared under the freeze–quench turnover conditions used for making the EPR samples in Figure 3. The total concentration of ammonia (NH_4^+ at pH 7.3) generated under 1 atm of N_2 is about 0.15 mM; that produced under 0.05 atm of N_2 is about 4–5-fold less (Figure S1). We then freeze trapped ***EG*** during turnover under 0.05 atm of N_2 in the presence of 0.2 mM of externally added NH_4^+, even more than the amount produced at 1 atm of N_2. There is no previous report of which we are aware that suggested the presence of NH_4^+ alters catalysis, and we find that added NH_4^+ has no influence on either the intensity of the EPR signal from trapped ***EG*** or the cryoannealing kinetics of ***EG*** (not shown). Hence we discard this possibility.

An influence of the diatomics N_2 and H_2 on $E_4(2N2H)$ decay is implicit in our mechanistic proposal that $E_4(2N2H)$ is formed by N_2 binding and H_2 release through *re*, Figure 1B. According to this mechanism, decay of ***EG*** would occur by the reverse of the *re* equilibrium (Scheme 1) and would involve oxidative addition (*oa*) of H_2 formed during turnover with release of N_2 to generate $E_4(4H)$. Hence, decay would be *enhanced* by increasing $[H_2]$; the $E_4(4H)$ thus formed by reaction with H_2 would in turn decay to E_0 through the successive release of two H_2. However, the $E_4(4H)$ can re-react with N_2 in the frozen solution to regenerate $E_4(2N2H)$, so increasing $[N_2]$ would *suppress* the decay. Thus, according to this *reversible-re* scenario, varying the concentrations $[H_2]$ and $[N_2]$ in frozen samples would *competitively* modulate both the accumulation and annealing of ***EG***.

According to this hypothesis, decay of $E_4(2N2H)$ is slower in samples prepared under high $P(N_2)$, Figure 3, because the $E_4(4H)$ state formed during $E_4(2N2H)$ decay undergoes enhanced regeneration back to $E_4(2N2H)$ through reaction with the high solution concentration of N_2 according to Scheme 1. Indeed, the measurements of $[N_2]$ in solution, Figure S3, show that $[N_2]$ in the solution prepared at $P(N_2)$ = 1 atm is more than an order of magnitude higher than that at 0.05 atm. This in turn correlates with the more than 10-fold slower decay of ***EG*** in the sample prepared under high $P(N_2)$, consistent with the expectation $E_4(2N2H)$ decay is being *suppressed* by enhanced re-reaction of $E_4(4H)$ with dissolved N_2 to regenerate $E_4(2N2H)$. One might imagine that the difference in decay rates of Figure 3 reflects the reaction of $E_4(2N2H)$ with differing concentrations of H_2 formed during turnover under the different values of $P(N_2)$. However, experiments described in SI argue against this alternative. Although more H_2 is produced during turnover under low $P(N_2)$,[1−3] saturating concentrations of H_2 are produced by the enzymatic reaction under all partial pressures of N_2 used (Figure S2).

To test the *reversible-re* hypothesis in experiments where both $[H_2]$ and $[N_2]$ are actively varied, we complemented our standard procedures for sample preparation with the simple expedient of flushing the headspace with an N_2/Ar mixture of selected $P(N_2)$ while rapidly stirring, thereby sweeping out the enzymatically produced H_2 into the headspace over the reaction mixture and generating samples with low $[H_2]$, while ensuring equilibration of the reaction mixture with the selected $P(N_2)$ in the headspace gas phase. Stirred and unstirred sample pairs prepared with the same $P(N_2)$ have essentially the same $[N_2]$, but the unstirred samples have high (saturating) $[H_2]$, while the stirred samples have low $[H_2]$.

Figure 4 presents the results of −50 °C cryoannealing of two stirred/unstirred pairs of samples of intermediate ***EG*** freeze-trapped during steady-state turnover. One pair was trapped under $P(N_2)$ = 0.1 and 0.9 atm of Ar; the second pair was freeze-trapped under $P(N_2)$ = 1 atm. Comparison of decay curves for sample pairs with high vs low $P(N_2)$, both the stirred and the unstirred pairs, again shows that high $[N_2]$ *suppresses*

DOI: 10.1021/jacs.5b00103
J. Am. Chem. Soc. 2015, 137, 3610–3615

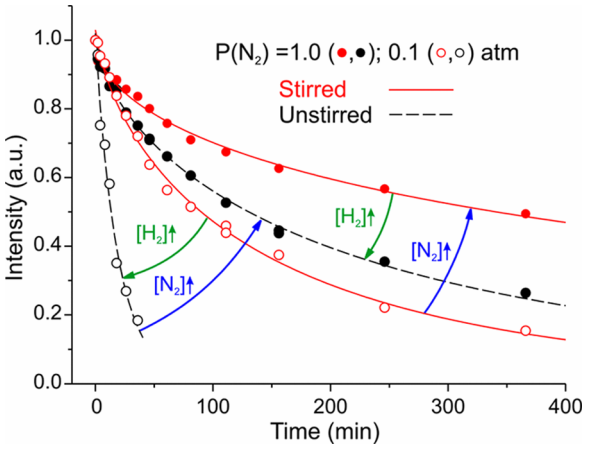

Figure 4. Progress curves for −50 °C cryoannealing of ***EG*** intermediates formed during turnover under $P(N_2)$ = 0.1 (open circles) and 1 (closed circles) atm, with (red) or without (black) stirring reaction mixture. Blue arrows connect pairs of samples prepared with different $P(N_2)$, with arrow pointing toward higher solution $[N_2]$, namely $P(N_2)$ = 1 atm; within a pair, $[H_2]$ is comparable, either low because in both samples enzymatically produced H_2 has been flushed out by stirring, or high in unstirred samples. Green arrows connect pairs of samples prepared under the same $P(N_2)$, and thus with comparable $[N_2]$ (either low because $P(N_2)$ = 0.1 atm or high, $P(N_2)$ = 1 atm) but different $[H_2]$, with arrow pointing from sample in which $[H_2]$ is low because stirring has flushed out the H_2 into the headspace, toward unstirred sample with higher $[H_2]$. Intensities measured as described in Figure 3A. Decays are fit as stretched exponentials (eq 2) with the parameters in Table 1.

Table 1. Parameters for the Stretched Exponentials from Eq 2, Used in Fitting the Decays in Figure 4

	$P(N_2)$ = 0.1 atm		$P(N_2)$ = 1 atm	
turnover conditions	unstirred	stirred	unstirred	stirred
τ (min)	19	142	224	667
m	0.94	0.71	0.68	0.55

E_4(2N2H) decay, regardless of whether the solution contains high $[H_2]$ (unstirred) or low (stirred).[25] Conversely, the effects of stirring on samples prepared under equal $P(N_2)$ show that the higher $[H_2]$ in the unstirred partner of a pair with identical $P(N_2)$ *speeds* the decay, regardless of whether $[N_2]$ is high ($P(N_2)$ = 1 atm) or low (0.1 atm).

Examination of Figure 1 shows that these effects clearly identify ***EG*** as E_4(2N2H). Considering the other E_n, $n \geq 4$, *even*, states, as noted above, E_8 has already been identified with intermediate ***I***, and in any case would not respond to changes in $[N_2]$ or $[H_2]$. Whether E_6, which we have assigned as binding N_2H_4,[8,10] decayed by loss of N_2H_4 or through the release of N_2H_2 and H_2, it would not respond to changes in $[N_2]$, and increasing $[H_2]$ would not speed its decay. Moreover, even in an alternative reaction pathway that has been discussed,[8,10] where E_6 contains a moiety generated by cleavage of the N−N bond, here too its decay could not be influenced by changes in $[N_2]$ or $[H_2]$. Instead, Figure 1 shows that the effects of the two diatomics clearly require not only that ***EG*** is E_4(2N2H), but also that its decay, Figures 3 and 4, is to be understood as the reverse of the *re* activation equilibrium,

$$E_4(4H) + N_2 \rightleftharpoons E_4(2N2H) + H_2 \quad (4)$$

which leads to the decay of E_4(2N2H) through Scheme 1: the *oa* reaction of E_4(2N2H) with H_2 and loss of N_2 to form E_4(4H) (k_b). The competing regeneration of E_4(2N2H) from E_4(4H) through reaction with N_2 (k_r) and *re* of H_2, in turn competes with the irreversible relaxation of E_4(4H) through loss of H_2 (k_d). This competition is captured by a steady-state treatment of the concentration of E_4(4H) within the kinetic relaxation Scheme 1, which generates as the functional form for $k_1(t)$, the observed rate constant of E_4(2N2H) relaxation according to eq 3,[26]

$$k_1(t) = \left(\frac{k_d k_b[H_2]}{k_r[N_2] + k_d}\right) \quad (5a)$$

In the limit of eq 5a where $k_d \ll k_r[N_2]$, the two states E_4(2N2H) and E_4(4H) are in an equilibrium controlled by the ratio, $[H_2]/[N_2]$; the equilibrium population decays to E_2(2H) with loss of H_2, with rate constant $k_1(t)$ represented by the limiting form of eq 5b,

$$k_1(t) \approx \left(\frac{k_d k_b[H_2]}{k_r[N_2]}\right) \propto \frac{[H_2]}{[N_2]} \quad (5b)$$

in agreement with the behavior exhibited in the present experiments, Figure 4. The rate constant $k_1(t)$ is expected to be time-dependent because the distribution of rate constants that characterizes a stretched-exponential decay in the frozen solid[23] is manifest as a time-dependent rate constant;[24] time dependence of the concentrations of the diatomics during annealing of the frozen solutions would also contribute. If conditions can be established such that E_4(4H) is trapped in quantities that allow k_d for wild-type nitrogenase to be measured directly, then the equilibrium constant of *re* (Figure 1B, eq 4), (k_r/k_b) in Scheme 1, can be estimated from eq 5b.

We also studied the effects of varying $[H_2]$ and $[N_2]$ on the *amount* of ***EG***/E_4(2N2H) trapped through the preparation of paired samples, with and without stirring/flushing, under a range of N_2 partial pressures, Figure 5. At the low partial

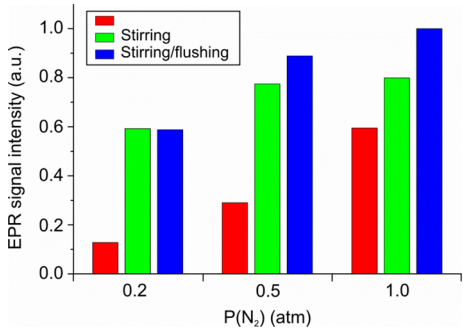

Figure 5. Variation in the EPR amplitude of trapped intermediate ***EG*** g_1 feature at various N_2 partial pressures when reaction mixture is neither stirred nor flushed (red); stirred (green); stirred with the headspace of reaction vial flushed with appropriate N_2/Ar mixture during turnover. EPR conditions: as described in Figure 3A.

pressure of $P(N_2)$ = 0.2 atm, stirring/flushing to remove H_2 increases the concentration of trapped ***EG*** by ∼4−5 fold. However, as the partial pressure of N_2 substrate rises, the significance of stirring/flushing drops, and by 1 atm N_2 the increase is less than 2-fold. The improved yield of ***EG*** by stirring/flushing effect can be easily explained by the effect of changes of $[H_2]$ and $[N_2]$ on the competition of H_2 with N_2 for

DOI: 10.1021/jacs.5b00103
J. Am. Chem. Soc. 2015, 137, 3610−3615

binding to the different E_4 substates, as shown in Figure 1B and eq 4. Under all partial pressures employed, a saturating level of H_2 is generated in the unstirred sample (Figure S2), so the removal of H_2 by stirring/flushing would have (roughly) the same influence for all samples. However, the majority of dissolved N_2 is used up before freezing when $P(N_2)$ is low, but there is considerable residual N_2 at the time of freezing for high $P(N_2)$ (Figure S3). Thus, the equilibration of the gaseous and solution N_2 has a lesser effect at high $P(N_2)$.

CONCLUSIONS

EPR/ENDOR spectroscopy has shown that the $S = {}^1/_2$ intermediate ***EG*** freeze-trapped during turnover of nitrogenase under N_2 contains N_2 or a reduction product bound to FeMo-co.[17−19] This implies that the intermediate must be an E_n state with n = 4, 6, or 8. Cryoannealing experiments on ***EG*** prepared under turnover conditions in which the concentrations, $[H_2]$, $[N_2]$ are systematically varied demonstrate that reaction of ***EG*** with the H_2 produced during turnover enhances the decay of ***EG*** and limits its accumulation, whereas reaction of N_2 with E_4(4H) formed during the decay process slows the observed decay of ***EG***. In the kinetic scheme of Figure 1A there is only one such state that could be affected by H_2, namely E_4(2N2H), the key catalytic intermediate formed upon *re* of H_2 and binding of N_2 (Figure 1B), whose decay involves the $[H_2]$, $[N_2]$ diatomics through the process visualized in Scheme 1. ***EG***/E_4(2N2H) is a state in which FeMo-co binds the components of diazene, which may be present as N_2 and two $[e^-/H^+]$ or as diazene itself, an issue to be addressed by future ENDOR measurements. Overall, however, the freeze-quench strategy nonetheless has trapped three of the five intermediate states in which N_2 is involved: one of the substates of E_4, E_7, and E_8,[5,7−9] leaving only E_5 and E_6 unexamined.

Of primary importance, the present finding that decay of ***EG*** is accelerated by increasing $[H_2]$ and slowed by increasing $[N_2]$ in the frozen reaction mixture, and the resulting identification of ***EG*** as E_4(2N2H) directly demonstrates that activation of nitrogenase for N_2 binding and reduction involves the thermodynamically and kinetically reversible reductive-elimination/oxidative-addition activation equilibrium of Figure 1B and eq 4, as previously inferred,[11] with its implied limiting stoichiometry of eight electrons/protons for the reduction of N_2 to two NH_3 (eq 1).

ASSOCIATED CONTENT

Supporting Information

Details of activity assays and of the estimation of H_2 and N_2 concentration in frozen EPR samples (three figures). This material is available free of charge via the Internet at http://pubs.acs.org.

AUTHOR INFORMATION

Corresponding Authors

*deandr@vbi.vt.edu
*lance.seefeldt@usu.edu
*bmh@northwestern.edu

Author Contributions

‖D.L. and Z.-Y.Y. made equal contributions to this work.

Notes

The authors declare no competing financial interest.

ACKNOWLEDGMENTS

This material is based upon work supported by the NIH (GM 111097, B.M.H.) and the U.S. Department of Energy, Office of Science, Office of Basic Energy Sciences (L.C.S. and D.R.D.).

REFERENCES

(1) Burgess, B. K.; Lowe, D. J. *Chem. Rev.* **1996**, *96*, 2983.
(2) Thorneley, R. N. F.; Lowe, D. J. *Metal Ions Biol.* **1985**, *7*, 221.
(3) Simpson, F. B.; Burris, R. H. *Science* **1984**, *224*, 1095.
(4) Wilson, P. E.; Nyborg, A. C.; Watt, G. D. *Biophys. Chem.* **2001**, *91*, 281.
(5) Igarashi, R. Y.; Laryukhin, M.; Dos Santos, P. C.; Lee, H. I.; Dean, D. R.; Seefeldt, L. C.; Hoffman, B. M. *J. Am. Chem. Soc.* **2005**, *127*, 6231.
(6) Lukoyanov, D.; Barney, B. M.; Dean, D. R.; Seefeldt, L. C.; Hoffman, B. M. *Proc. Natl. Acad. Sci. U.S.A.* **2007**, *104*, 1451.
(7) Lukoyanov, D.; Yang, Z.-Y.; Dean, D. R.; Seefeldt, L. C.; Hoffman, B. M. *J. Am. Chem. Soc.* **2010**, *132*, 2526.
(8) Hoffman, B. M.; Lukoyanov, D.; Dean, D. R.; Seefeldt, L. C. *Acc. Chem. Res.* **2013**, *46*, 587.
(9) Doan, P. E.; Telser, J.; Barney, B. M.; Igarashi, R. Y.; Dean, D. R.; Seefeldt, L. C.; Hoffman, B. M. *J. Am. Chem. Soc.* **2011**, *133*, 17329.
(10) Hoffman, B. M.; Lukoyanov, D.; Yang, Z.-Y.; Dean, D. R.; Seefeldt, L. C. *Chem. Rev.* **2014**, *114*, 4041.
(11) Yang, Z.-Y.; Khadka, N.; Lukoyanov, D.; Hoffman, B. M.; Dean, D. R.; Seefeldt, L. C. *Proc. Natl. Acad. Sci. U.S.A.* **2013**, *110*, 16327.
(12) Crabtree, R. H. *The Organometallic Chemistry of the Transition Metals*, 5th ed.; Wiley: Hoboken, NJ, 2009.
(13) Ballmann, J.; Munha, R. F.; Fryzuk, M. D. *Chem. Commun.* **2010**, *46*, 1013.
(14) Kubas, G. J. *Chem. Rev.* **2007**, *107*, 4152.
(15) Peruzzini, M., Poli, R., Eds. *Recent Advances in Hydride Chemistry*; Elsevier Science B.V.: Amsterdam, The Netherlands, 2001.
(16) Shaw, S.; Lukoyanov, D.; Danyal, K.; Dean, D. R.; Hoffman, B. M.; Seefeldt, L. C. *J. Am. Chem. Soc.* **2014**, *136*, 12776.
(17) Seefeldt, L. C.; Hoffman, B. M.; Dean, D. R. *Annu. Rev. Biochem.* **2009**, *78*, 701.
(18) Barney, B. M.; Lukoyanov, D.; Igarashi, R. Y.; Laryukhin, M.; Yang, T.-C.; Dean, D. R.; Hoffman, B. M.; Seefeldt, L. C. *Biochemistry* **2009**, *48*, 9094.
(19) Barney, B. M.; Yang, T.-C.; Igarashi, R. Y.; Santos, P. C. D.; Laryukhin, M.; Lee, H.-I.; Hoffman, B. M.; Dean, D. R.; Seefeldt, L. C. *J. Am. Chem. Soc.* **2005**, *127*, 14960.
(20) Lukoyanov, D.; Dikanov, S. A.; Yang, Z.-Y.; Barney, B. M.; Samoilova, R. I.; Narasimhulu, K. V.; Dean, D. R.; Seefeldt, L. C.; Hoffman, B. M. *J. Am. Chem. Soc.* **2011**, *133*, 11655.
(21) Lukoyanov, D.; Yang, Z.-Y.; Duval, S.; Danyal, K.; Dean, D. R.; Seefeldt, L. C.; Hoffman, B. M. *Inorg. Chem.* **2014**, *53*, 3688.
(22) Christiansen, J.; Goodwin, P. J.; Lanzilotta, W. N.; Seefeldt, L. C.; Dean, D. R. *Biochemistry* **1998**, *37*, 12611.
(23) Davydov, R.; Hoffman, B. M. *Arch. Biochem. Biophys.* **2011**, *507*, 36.
(24) Phillips, J. C. *Rep. Prog. Phys.* **1996**, *59*, 1133.
(25) Although $[N_2]$ is somewhat depleted in the unstirred samples relative to that of the stirred samples, the effect is minimal in this context (SI).
(26) For completeness, we might add to $k_1(t)$ a rate constant $k_0(t)$ that is independent of diatomic concentrations and represents the possibility of "simple" loss of N_2 and stepwise return to ground. However, the observed control of the decay by $[H_2]/[N_2]$ shows that such a process, if operative at all, cannot be making a significant contribution.

DOI: 10.1021/jacs.5b00103
J. Am. Chem. Soc. 2015, 137, 3610−3615